High-efficiency dye-sensitized solar cells with molecular copper phenanthroline as solid hole conductor

Supporting Information

1. **Synthesis of copper 2,2'-dimethyl phenanthroline ($Cu^{(I/II)}(dmp)_2TFSI_{1/2}$)**
$Cu^{(I/II)}(dmp)_2TFSI_{1/2}$(3): All chemicals and solvents were purchased from Sigma-Aldrich, if not stated otherwise, and were used without further purification.
For ($Cu(dmp)_2Cl_2$ 1), **o**ne equivalent of $CuCl_2$ was mixed with 4 equivalents of Neocuproine hydrate in ethanol, under nitrogen atmosphere, at room temperature for 2 hours. Complex (1) was collected by filtration and washed with water and diethyl ether. The yield was 80 % (mol). Cu(II)$(dmp)_2$Cl/TFSI (2): Complex (1) was dissolved in a 1:2 ethanol/water mixture. To this solution, 5 equivalents of LiTFSI were added. The solution was stirred for 2 hours at room temperature under nitrogen atmosphere. Complex (2) was collected by filtration and washed with water and diethyl ether. The yield was 92 % (mol). Cu(I)dmp2TFSI (3): Complex (2) was dissolved in acetonitrile. To this solution, 10 equivalents of ascorbic acid were added. The solution was stirred for 2 hours at room temperature under nitrogen atmosphere in diethyl ether. After filtration of the remaining ascorbic acid, the solvent was evaporated which provided complex (3) as a crude of dark red powder. After further purification, complex (3) was obtained as intense red powder. The yield was 90 % (mol).

^{1}H NMR (400 MHz, acetone d6): δ 8.75 (d, *J*(H–H) = 8.21 Hz, 1H), 8.23 (s, 1H), 7.98 (d, *J*(H–H)= 8.24 Hz, 1H), 2.52 (s, 3H).

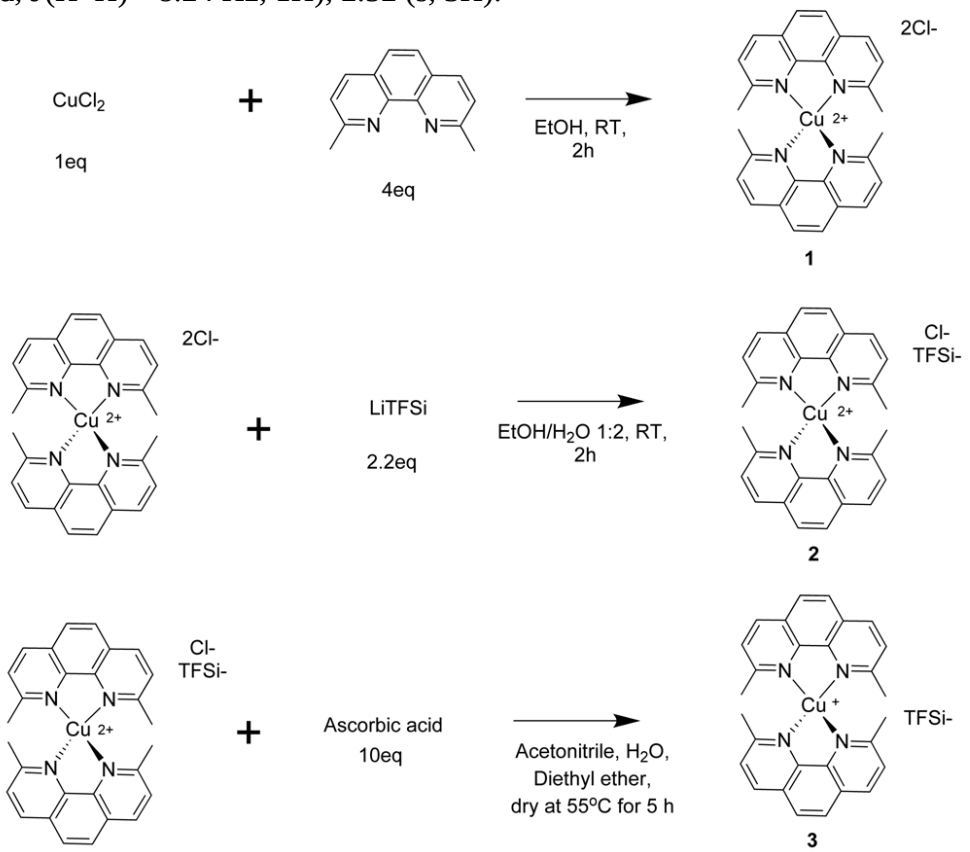

Scheme S 1 Synthetic Procedure for $Cu^{(I/II)}(dmp)_2$TFSI/Cl (2 and 3)

2. XRD of ssDSC working electrode

By solving the copper complex in a solvent, the hole conductor layer have deposited on the working electrode using spin coating or drop casting methods. Self assembly/alignment of copper complexes in between the dye sensitized mesoporous TiO_2 layer and on the top of it (called capping layer) is different for different solvents or casting methods. The differences can be investigated by X-ray diffraction (XRD) patterns of hole conductor layer (Fig. S1). 20 different solvents have been tested (data are not shown) in which each solvent results in special XRD pattern for hole conductor layer.

Drying of electrolyte in the zombie cells could result in a porous hole conductor layer between the working/counter electrodes (considering at least 20 micrometer distance between two electrodes). On the other hand, in a solid state device we have a few micrometer dense hole conductor layer which results in a different XRD pattern. Spin coating of acetonitrile solution has not any crystalline peak while drop casting with subsequent slow drying in air shows crystalline structure (Fig. S1) in which some needles in the capping layer are observable by naked eye.

In a Zombie cell drying process, we can expect fast evaporation of acetonitrile from liquid electrolyte with subsequent self assembly of copper complexes in the presence of Tbp solvent. Comparison of XRD pattern of a Zombie cell working electrode with air dried acetonitrile or Tbp solutions reveal the following distinguishable features which can be responsible partly for different performances of corresponding devices:

1- There are two peaks in 17 and 21 degrees (labelled by #) which is common for all cases (zombies-acetonitrile or Tbp air dried).
2- Two peaks of 11.5 and 14 degrees (labelled by *) are not present in zombie cells but exist in air dried cells.
3- There are some little shifts in the # peaks in different cells indicative of different possible chemical heterogeneities or dislocations.

Absence of * labelled peaks (fig. X) and the presence of a peak in 44 degree for Zombie cell is the main clues revealing the structural differences between the zombies and air dried samples. Therefore, possible energy band offsets can be present in different crystalline structures resulting in different dye regeneration/ hole hopping time constants.
Furthermore, XRD pattern of an opened liquid based device with subsequent drying in air (fig X) shows the presence of 14(* labelled) and 17(# labelled) degree peaks together with 44 degree zombie peak which is different from zombie pattern. Resolving of XRD spectra following the effect of different solvent/drying methods will uncover the mechanism of copper complexes self-assembly in the hole conducting layer.

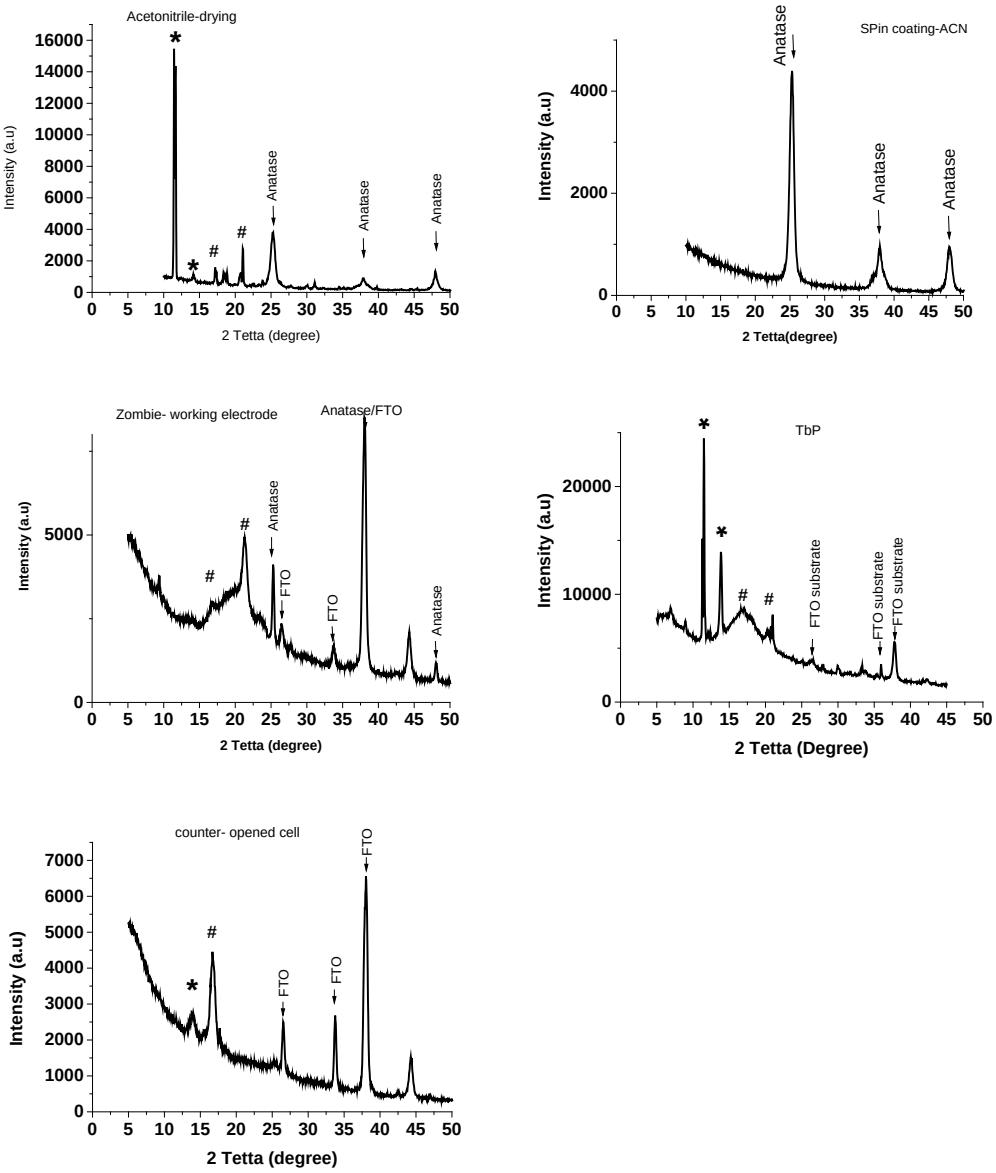

Figure S 1 XRD of ssDSC working electrodes, TiO_2 with $Cu(dmp)_2$ HTM

3. Charge extraction experiments in solar cells

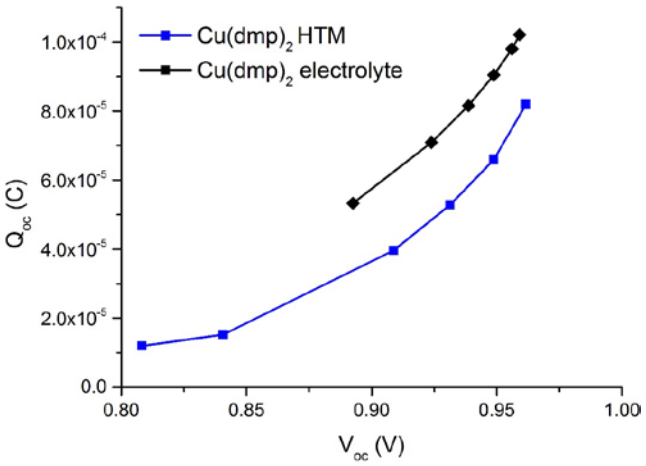

Figure S 2 Extracted charge as a function of V_{OC}

4. Cyclic Voltammetry

A three-electrode cell was used for the cyclic voltammetry experiments. The supporting electrolyte used for electrochemical measurements was 0.1 M $LiN(CF_3SO_2)_2$ in acetonitrile. The counter electrode is a stainless steel plate with an area of 3 cm^2. The reference electrode was Ag/AgCl; a salt bridge electrolyte was interposed between working and reference electrode, containing 0.1 M $LiN(CF_3SO_2)_2$ in acetonitrile. The reference electrode was calibrated by recording the cyclic voltammogram of ferrocene in the same electrolyte; the potential values are on the basis of the estimated value of the ferrocene redox potential in acetonitrile 0.624 V/SHE.[1] The formal potential $E^{0'}$ Cu(I/II)$(dmp)_2$ = 0.94 V vs SHE. For comparison, $E^{0'}(\text{spiro-OMeTAD}^{0/+})$= 0.76 V vs SHE (Ute B. Cappel, Elizabeth A. Gibson, Anders Hagfeldt, and Gerrit Boschloo , The Journal of Physical Chemistry C **2009** 113 (15), 6275-6281).

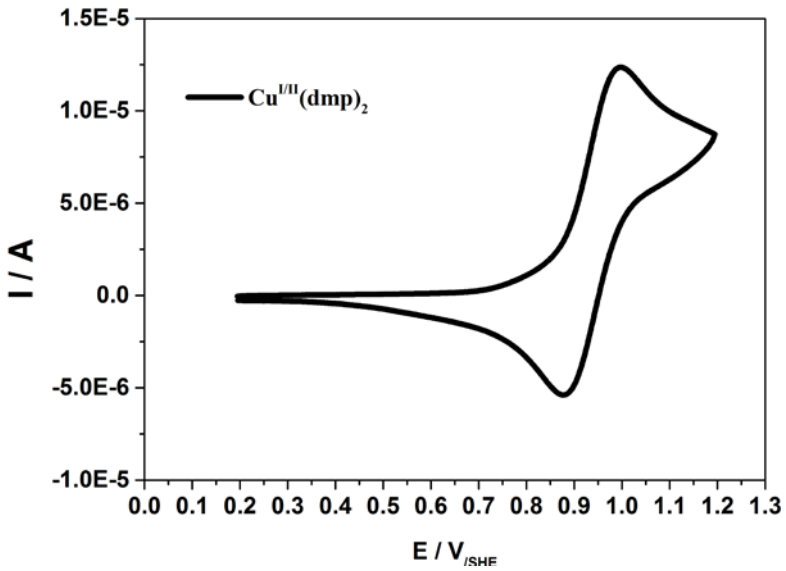

Figure S 3 Cyclic voltammogram of Cu(I/II)(dmp)$_2$TFSI/Cl: E^{0}'= 0.94 V vs SHE.

5. Distribution of Photovoltaic Performance

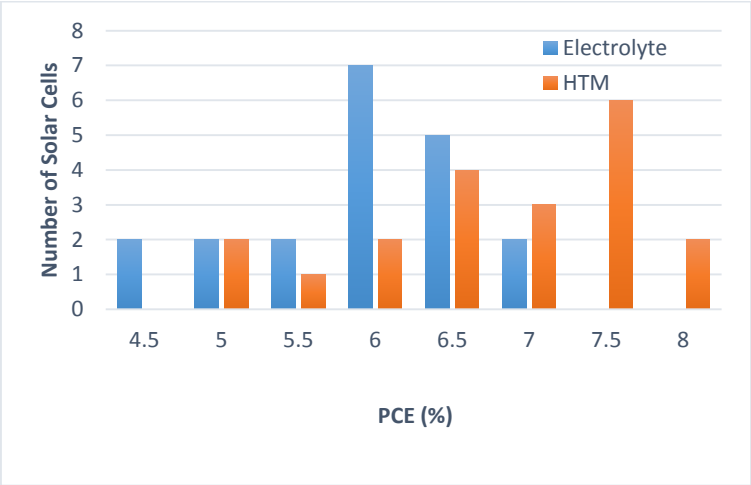

Figure S 4 Distribution of photovoltaic performance of 20 DSC and 20 ssDSC devices

6. Hole Mobility

The hole mobility of the material was measured by use of the space-charge limited current (SCLC) method. A HTM solution was spin-coated on top of a layer of PEDOT:PSS on FTO glass forming a sample with the structure FTO/PEDOT:PSS/HTM/Au. By measuring the current-voltage characteristics of the sample in dark the hole-mobility can be evaluated from the Mott-Gurney law for SCLC,

$$J(V) = \frac{9}{8}\varepsilon\varepsilon_0\mu\frac{V^2}{d^3} \qquad \text{Equation S1}$$

where ε is the dielectric constant of the material, ε_0 is the permettivity of vacuum, μ is the hole mobility, V is the applied bias and d is the film thickness. H. Snaith and M. Grätzel [3] noted that for most organic semiconductor the dielectric constant, ε, can be assumed to be 3. This was used in the case of $Cu^{I}(dmp)_2$ as it was found to be a good assumption.[3] The thicknesses of the spin-coated films are 200 and 800 nm for doped spiro-OMeTAD and neat $Cu^{I}(dmp)_2$ (without TBP, Li-TFSI), respectively.

Table S 1: Resulting conductivities and hole mobilities for doped spiro-OMeTAD and $Cu^{I}(dmp)_2$ as obtained from SCLC samples.

	Conductivity ($S\ cm^{-1}$)	Hole Mobility ($cm^2\ V^{-1}\ s^{-1}$)
Spiro-OMeTAD*	$2 \cdot 10^{-5}$	$4 \cdot 10^{-3}$
$Cu^{I}(dmp)_2$	$1 \cdot 10^{-5}$	$3 \cdot 10^{-2}$

* 65 mM in Chlorobenzene, with 32 mM Li-TFSI and 195 mM TBP.

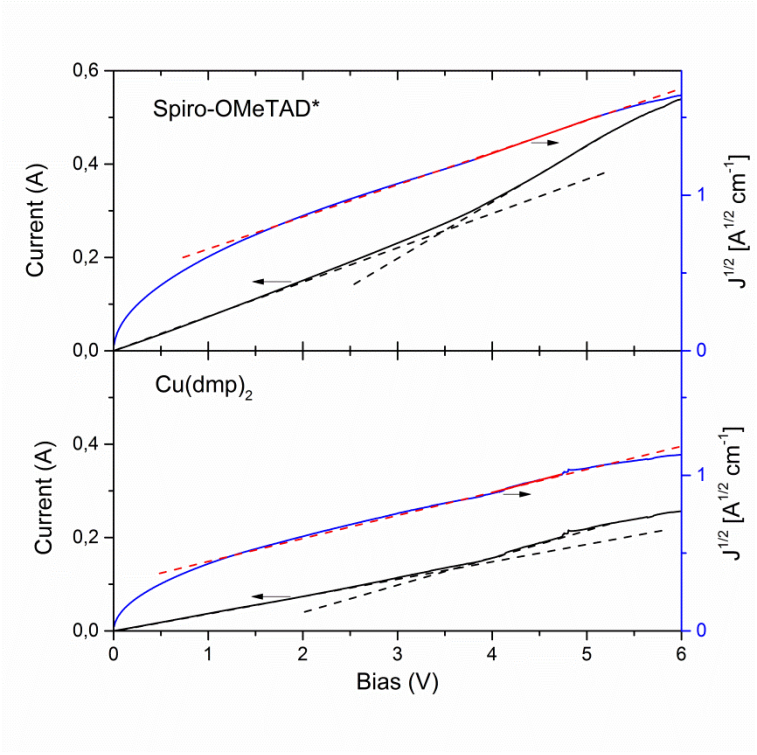

Figure S 5. IV characteristics for hole-mobility samples of spiro-OMeTAD doped with Li-TFSI and TBP additives (top) and $Cu^{I}(dmp)_2$ (bottom). Left axis (black) shows the current response and right axis (blue) shows the square-root of the current density. Black dashed lines serve as a guide for the eye to see the onset of the space charge limited current region. Red line shows the region which is linearly fitted to obtain hole mobilities.

7. Electron lifetime in spiro-OMeTAD-based ssDSC

For D35-sensitized ssDSC using spiro HTM, an electron lifetime of 3 ms at a V_{OC} of 0.95 V is reported by Jiang et al. (Adv. Funct. Mater. 2011, 21, 2944–2952). The TiO_2 thickness was 2.7 μm. Similar values have also been reported by Snaith and co-workers (see, e.g. Nanotechnology 19 (2008) 424003). Increasing the mesoporous TiO_2 film thickness will reduce the electron lifetime.

References

S1. Abe, H. & Miyamura, K. Monolayer formation and aggregation of nickel(II) complexes coordinated with salen substituted by non-linear alkyl side chains. *Inorganica Chim. Acta* **298,** 90–93 (2000).

S2. Snaith, H. J. & Grätzel, M. Enhanced charge mobility in a molecular hole transporter via addition of redox inactive ionic dopant: Implication to dye-sensitized solar cells. *Appl. Phys. Lett.* **89,** - (2006).

S3. Cappel, U. B., Daeneke, T. & Bach, U. Oxygen-Induced Doping of Spiro-MeOTAD in Solid-State Dye-Sensitized Solar Cells and Its Impact on Device Performance. *Nano Lett.* **12,** 4925–4931 (2012).